TAO, Vol.6, No.1, 129-150, March 1995

The Distributions of Calcareous Nannofossils and Grain Size in the Surface Sediments of the East China Sea and Their Relationship to the Current Pattern

MIN-PEN CHEN[1] and CHAO-KAI HUANG[1]

(Manuscript received 1 May 1994, in final form 16 December 1994)

ABSTRACT

Nannofossil assemblages, carbonate content and grain size distributions were analyzed in 46 samples of surface sediments collected in the middle and outer shelf of the East China Sea. Thirty three indigenous taxa were identified. *Emiliania huxleyi* **and** *Gephyrocapsa oceanica* **were the two dominant calcareous nannoplankton species. The former was derived from both the China Coastal Current and the Kuroshio Current. The latter originated mainly from the Japan longshore current. Sediments containing high carbonate content (>30%) were deposited along the shelf break of the East China Sea. About 80% of the total carbonate material was composed of shell fragments and foraminiferal tests. Nannofossils were found mainly in the south of the loop current off the Chagjiang River, the western tip of the Japan longshore current and in the western flank of the Okinawa Trough.**

The grain size distribution pattern can be divided into four types: a unimodal pattern in the fine grain material (about 10 μm) which is composed mainly of loess; a unimodal pattern occurrring in the coarse grain size (about 200-300 μm) which is composed mainly of foraminifera and shell fragments; a bimodal pattern with a higher concentration of fine sediment, and a bimodal pattern with less fine-grained sediment. The bimodal sediments are distributed between the two single modes. The finer carbonate-free sediment with bimodal size distribution is derived mainly from the Changjiang River. The coarse fractions are composed of terrigenous materials derived from either mainland China or from Taiwan.

From the factor analysis of ten selected nannofossil species and groups, the sediment transportation path of each current can be deduced from the factor loading contours. In the middle and outer shelf of the East China Sea, seven current tracks, including the main Kuroshio Current, a branch of the Kuroshio Current, the Taiwan Current, the loop current from Changjian, the China Coastal Current, the Tsushima Current and the longshore current from Japan are recognized.

(Key words: East China Sea, Surface Sediment, Nannofossil, Grain size, Current path)

[1] Institute of Oceanography, National Taiwan University, Taipei, Taiwan, R.O.C.

1. INTRODUCITON

The distribution of calcareous nannofossils in surface sediments has been a subject of intense interest in the Pacific Ocean (Geitzenauer *et al.*, 1976; McIntyre *et al.*, 1970; Roth and Berger, 1975; Roth and Coulbourn, 1982; Tanaka, 1991) since it may record the environmental conditions under which these nannofossils were produced in the overlying surface waters (Roth and Berger, 1975; Geitzenauer *et al.*, 1976; Loubere, 1982). However, the distribution may be modified by other processes thereby causing the relative abundance of the species in sediments not to always reflect a unique paleoceanographic variable such as temperature. One of these modifying processes is the current pattern (Fincham and Winter, 1989; Winter, 1985; Tanaka, 1991; Zhang and Siesser, 1986).

In the East China Sea, the distribution of the calcareous nannoplankton thanatocoenoses in the surface sediments has been studied by Wang and Min (1981), Wang and Samtleben (1983), Zhang and Siesser (1986). These studies were restricted to the inner shelf and to the estuary of the Changjiang (Yangtze River), and the conclusions were mostly qualitative. In fact, neither the critical factors controlling the distribution of the coccoliths nor the grain-size distribution in the surface sediments was presented in any detail. In this study, the authors try to : (1) determine the distribution of calcareous nannofossils in the surface sediments in the middle to outer shelf of the East China Sea, (2) relate the distribution of selected coccolith assemblages to the current pattern in the East China Sea, and (3) determine the grain-size distribution of the surface sediments in order to understand the sources of the surface sediments in the middle and outer shelf of the East China Sea.

2. STUDY AREA

The East China Sea is a marginal sea situated between approximately 24°N, 121°E and 33° N, 130°E. It may be subdivided into three regimes: the inner, middle and outer shelves, with boundaries conventionally located at the 50-, 100- and 150-m isobaths, respectively (Zhang and Siesser, 1986). A branch of the Kuroshio Current intrudes into the southeastern boundary of the East China Sea. The warm Kuroshio Current dominates the outer shelf of the East China Sea, the shelf break, the continenal slope and the deep waters of the Okinawa Trough (Chern *et al.*, 1990). Another warm current which comes through the Taiwan Strait influences the middle shelf. The China Coastal Current, which is hyposaline (less than $30^{o}/_{oo}$) and 6° to 10°C colder than the Kuroshio Current, flows southward over the inner and middle parts of the shelf and mixes with the highly saline (more than $34^{o}/_{oo}$) Kuroshio Current at the edge of the East China Sea (Chu, 1971; Fan, 1985). The Changjiang River transports a large amount of sediment (over 2000 tons per year) into the East China Sea (Zhang and Siesser, 1986). The concentration of suspended matter can reach as much as 1000 mg/l at the mouth of the Changjiang River and 5 mg/l in a belt which is almost parallel to the 50-m isobath (Yang and Milliman, 1983; Wang and Samtleben, 1983).

Forty-six surface sediments were collected at 49 stations by a grab sampler during the Russia-ROC collaborative cruise (Figure 1), "KEEPMASS EXPEDITION", in July, 1992. The locations and the water depths of these stations are listed in Table 1 and shown in Figure 2. Samples were not collected at Stations E19, E23, E34.

KEEP-MASS Expedition Ship Track and Sampling Stations
July 10 - Aug. 5, 1992 by *R/V "Vinogradov"*

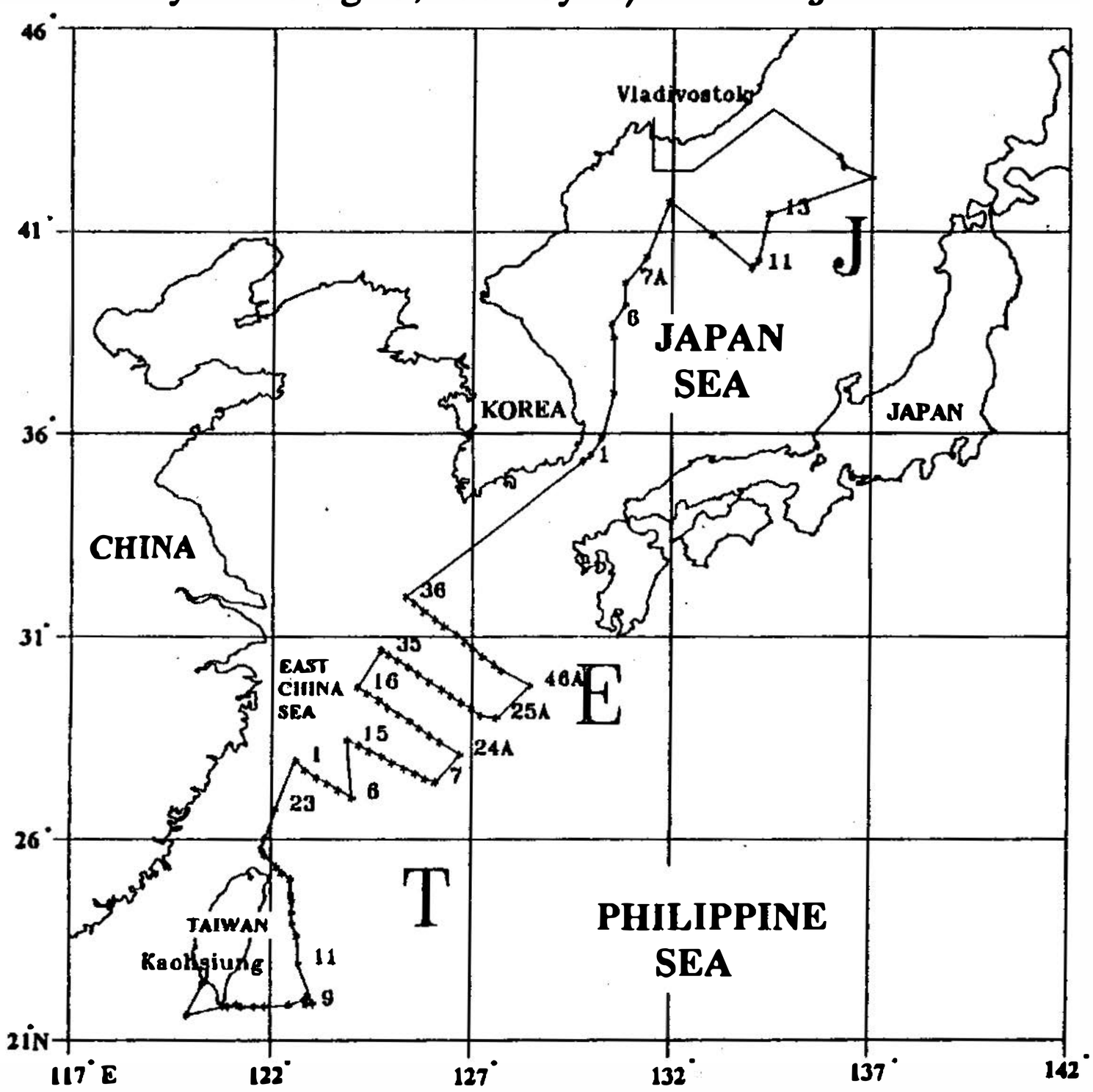

Fig. 1. Location of sampling stations during the ROC-Russia "KEEPMASS" collaboration expedition in 1992.

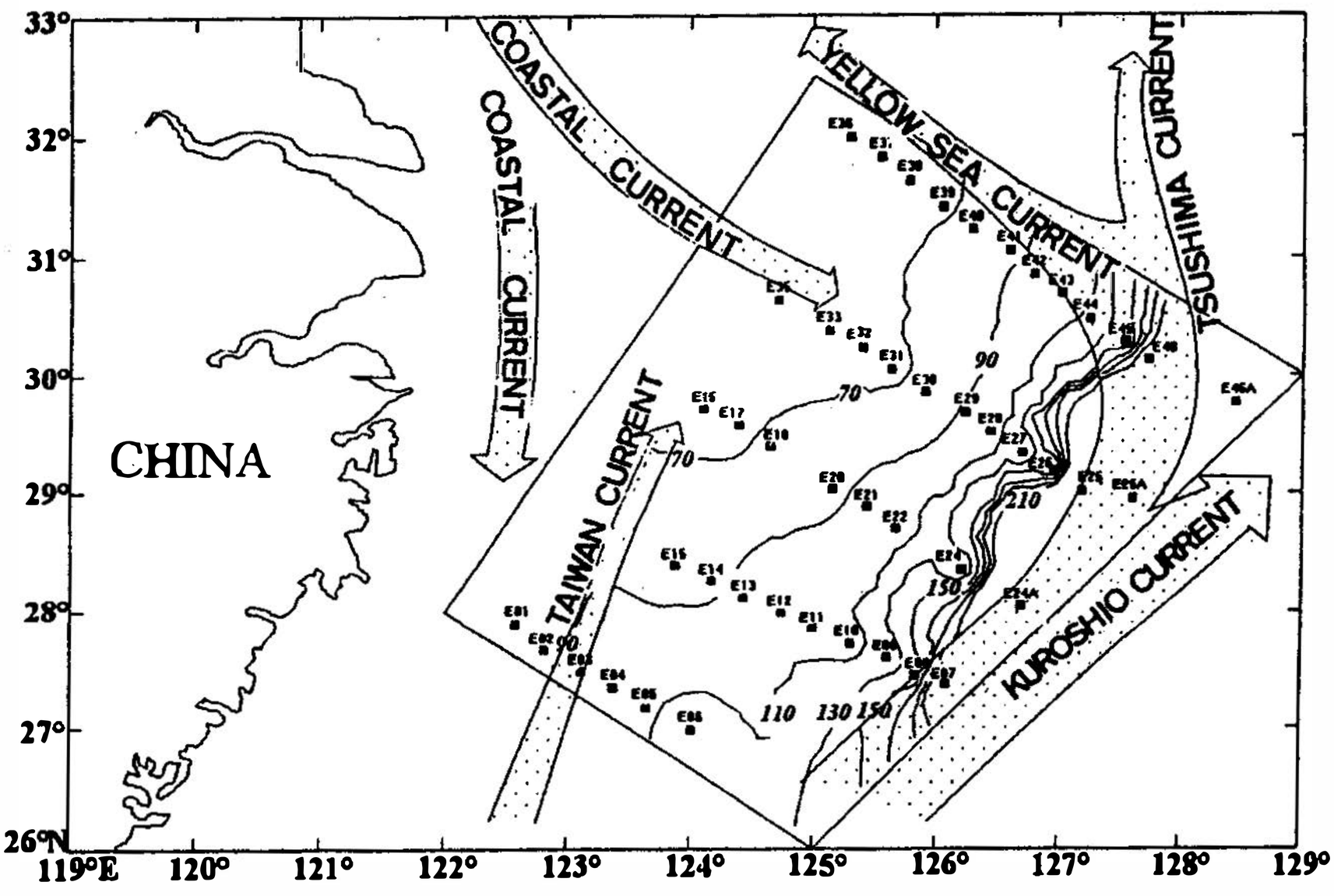

Fig. 2. Localities of sampling stations on the East China Sea. The current pattern was drawn from Zhang and Siesser (1986).

Table 1. The grab sampling locations and water depth in the East China Sea.

Sampling Station No.	Water Depth (m)	Longitude (E)	Latitude (N)
E1	72	122°35.34'	27°54.37'
E2	82	122°49.80'	27°40.95'
E3	103	123°07.26'	27°29.20'
E4	104	123°22.92'	27°20.84'
E5	110	123°39.72'	27°11.23'
E6	121	124°00.54'	26°59.74'
E7	330	126°05.16'	27°22.84'
E8	123	125°50.76'	27°27.19'
E9	113	125°35.82'	27°36.01'
E10	101	125°18.06'	27°44.06'
E11	104	124°59.94'	27°51.65'
E12	104	124°44.16'	28°00.68'
E13	96	124°26.34'	28°08.41'
E14	84	124°10.32'	28°17.03'
E15	79	123°52.92'	28°25.01'
E16	60	124°07.14'	29°43.81'
E17	64	124°22.68'	29°34.84'
E18	74	124°38.82'	29°24.80'
E19	81	124°52.43'	29°14.58'
E20	78	125°09.18'	29°03.13'
E21	102	125°26.22'	28°53.58'
E22	104	125°40.92'	28°42.95'
E23	108	125°56.15'	28°31.87'
E24	114	126°11.70'	28°22.48'
E24A	440	126°41.40'	28°03.76'
E25	390	127°12.12'	29°01.69'
E25A	1090	127°36.72'	28°57.77'
E26	122	126°57.60'	29°12.25'
E27	108	126°42.36'	29°21.08'
E28	100	126°26.40'	29°31.93'
E29	90	126°14.10'	29°41.25'
E30	77	125°54.54'	29°52.27'
E31	64	125°38.46'	30°03.55'
E32	69	125°23.82'	30°14.38'
E33	66	125°07.74'	30°23.68'
E34	52	124°54.08'	30°32.31'
E35	53	124°42.42'	30°39.46'
E36	51	125°18.42'	31°59.97'
E37	58	125°32.46'	31°50.52'
E38	60	125°46.74'	31°37.77'
E39	67	126°03.48'	31°25.96'
E40	78	126°17.22'	31°14.74'
E41	86	126°36.06'	31°03.56'
E42	96	126°47.82'	30°52.58'
E43	96	127°00.72'	30°42.52'

Table 1. (Continued)

Sampling Station No.	Water Depth (m)	Longitude (E)	Latitude (N)
E44	110	127°15.24'	30°29.83'
E45	128	127°32.82'	30°17.62'
E46	228	127°43.20'	30°09.14'
E46A	888	128°27.00'	29°46.91'

3. METHODS

Samples were prepared for the examination of calcareous nannoplankton using the standard settling technique. The slide was mounted with the Entellan for examination by light microscopy. Nannofossils were examined at a magnification of ×1,500. More than 300 specimens were identified and counted for each slide at random. Some samples were also studied by a scanning electron microscope (SEM) to identify and study the morphologies of the coccoliths in detail.

A description of the surface sediment is listed in Table 2. The surface sediments vary in lithology from clay to sand, and the grain size is independent of the water depth. Calcareous nannofossil species found in the studied samples are listed in Table 3 in which the species are listed according to the alphabetical order of genus epithets.

A laser particle size analyzer, the "ANALYSETTE 22", was used to measure the grain size distribution in the samples within the grain-size range of 0.16 to 1000 μm. For coarser particles (larger than 1000 μm), the grain size was measured by sieving.

The carbonate content was determined by the weight loss method outlined by Molnia (1974). Before the carbonate material was dissolved with 1N hydrochloric acid, the salt was removed by washing the sample in distilled water (Chen *et al.*, 1992). The laser particle size analyzer, the "ANALYSETTE 22", was also used to determine the size distribution of the carbonate-free residual.

4. RELATIVE ABUNDANCE AND DISTRIBUTION OF COCCOLITHIN SURFACE SEDIMENTS

The distribution of the carbonate content in the surface sediments of the study area is shown in Figure 3. The coarser carbonate material (>50 μm) is composed mainly of foraminiferal and shell fragments. The finer size (<50 μm) can be divided into fine bioclasts and coccoliths. The distribution of these finer particles is indicative of the distribution of the coccoliths (Figure 3). Concentrations exceeding 10% of the total carbonate content were found in the northern corner of the study area, and they may represent material from Huanghe, which transports eroded loess with carbonate contents of up to 15% (Qin and Li, 1983). Since marine biogenic carbonate may be added to the sediment during or after the transport of the particles, a high carbonate content in the sediment can only be used as a very general indicator (Li, *et al.*, 1991; Zhang, 1988; Zhu and Wang, 1988). Higher concentrations of coccoliths are found in two areas: in the lower middle portion of the studied area, and in the Okinawa Trough at the northeastern corner of the area (Figure 3). Zhang and Siesser (1986) also reported the occurrence of fewer coccoliths in the inner-shelf sediments and the progressive

Table 2. Surface Sediment Description of the East China Sea.

Core No.	Grain Size	Mineral Composition	Biogenic Composition	Rock Fragments
E1	Medium Sand	Qtz, Green Minerals 50%	Planktonic & Benthic Fora 10%	Sedimentary Rock 40%
E2	Medium Sand	Qtz, Green Minerals, Feldspar, 50%	Planktonic & Benthic Fora, Mollusca, 25%	Sedimentary Rock & Slate 25%
E3	Medium Sand	Qtz, Green Minerals 40%	Planktonic & Benthic Fora, Mollusca, 40%	Sedimentary Rock & Slate 20%
E4	Medium-Coarse Sand	Qtz, Green Minerals 30%	Planktonic & Benthic Fora, Mollusca, 55%	Sedimentary Rock & Slate 15%
E5	Medium-Coarse Sand	Qtz, Green Minerals 20%	Planktonic & Benthic Fora, Mollusca, 70%	Sedimentary Rock & Slate 10%
E6	Medium-Coarse Sand	Qtz, 20%	Planktonic & Benthic Fora, Mollusca, 60%	Sedimentary Rock 20%
E7	Medium-Coarse Sand	Qtz, Light Green Minerals, Feld, 50%	Planktonic & Benthic Fora, Mollusca, 30%	Sedimentary Rock & Slate 20%
E8	Medium Sand	Qtz, Feldspar 70%	Planktonic & Benthic Fora, Mollusca, 10%	Sedimentary Rock & Slate 20%
E9	Medium-Coarse Sand	Qtz, Feldspar 70%	Planktonic & Benthic Fora, Mollusca, 5%	Sedimentary Rock & Slate 25%
E10	Medium Sand	Qtz, Feld, Green & Dark Minerals, 50%	Planktonic & Benthic Fora 40%	Sedimentary Rock & Slate 10%
E11	Muddy Sand	Qtz, Feldspar 15%	Planktonic & Benthic Fora, Mollusca, 75%	Sedimentary Rock & Slate 10%
E12	Medium Sand	Qtz, 10%	Planktonic & Benthic Fora, Mollusca, 80%	Sedimentary Rock & Slate 10%
E13	Muddy Sand	Qtz, Light Green & Dark Minerals, 40%	Planktonic & Benthic Fora, Mollusca, 50%	Sedimentary Rock & Slate 10%
E14	Muddy Sand	Qtz, Feld, Green Minerals, 45%	Planktonic & Benthic Fora, Mollusca, 25%	Sedimentary Rock & Slate 30%
E15	Muddy Sand	Qtz, Feld, Light Green Minerals, 60%	Planktonic & Benthic Fora, Mollusca, 10%	Sedimentary Rock & Slate 30%
E16	Muddy Sand	Qtz, Feldspar 65%	Benthic Fora & Mollusca, 5%	Sedimentary Rock & Slate 30%
E17	Muddy Sand	Qtz, Light Green Minerals, 70%	Planktonic & Benthic Fora, Mollusca, 5%	Sedimentary Rock & Slate 25%
E18	Muddy Sand	Qtz, Feld, Light Green Minerals, 55%	Planktonic & Benthic Fora, Mollusca, 20%	Sedimentary Rock & Slate 25%
E20	Muddy Sand	Qtz, Feldspar, 50%	Planktonic & Benthic Fora, Mollusca, 30%	Sedimentary Rock & Slate 20%
E21	Muddy Sand	Qtz, Brown, Green & Dark Minerals, 60%	Planktonic & Benthic Fora, Mollusca, 25%	Sedimentary Rock & Slate 15%
E22	Muddy Sand	Qtz, Brown, Green & Dark Minerals, 60%	Planktonic & Benthic Fora, Mollusca, 25%	Sedimentary Rock & Slate 15%
E24	Muddy Sand	Qtz, Feld, Green Minerals, 35%	Planktonic & Benthic Fora, Mollusca, 50%	Sedimentary Rock & Slate 15%

Table 2. (Continued)

E25	Muddy Sand	None	Planktonic & Benthic Fora, Mollusca, 95%	Sedimentary Rock & Slate 5%
E26	Medium-Coarse Sand	Qtz, Muscovite, etc, 70%	Planktonic & Benthic Fora, Mollusca, 15%	Sedimentary Rock & Slate 15%
E27	Medium-Coarse Sand	Qtz, Feldspar, 50%	Planktonic & Benthic Fora, Mollusca, 30%	Sedimentary Rock 20%
E28	Medium-Coarse Sand	Qtz, Feld, Green & Dark Minerals, 50%	Planktonic & Benthic Fora, Mollusca, 25%	Sedimentary Rock 25%
E29	Medium Sand	Qtz, Feld, Light Green Minerals, 65%	Planktonic & Benthic Fora, Mollusca, 10%	Sedimentary Rock & Slate 25%
E30	Muddy Sand	Qtz, Light Green Minerals, 65%	Benthic Fora & Mollusca, 10%	Sedimentary Rock & Slate 25%
E31	Muddy Sand	Qtz, Feldspar, 60%	Benthic Fora & Mollusca, 10%	Sedimentary Rock 30%
E32	Muddy Sand	Qtz, Light Green Minerals, Mica, 40%	Planktonic & Benthic Fora, Mullusca, Ostrocod, 30%	Sedimentary Rock & Slate 30%
E33	Muddy Sand	Qtz, Light Green Minerals, Mica, 50%	Planktonic & Benthic Fora, Mullusca, Ostrocod, 25%	Sedimentary Rock & Slate 25%
E35	Muddy Sand	Qtz,Feld, Light Green Minerals, 50%	Planktonic & Benthic Fora, Mollusca, 15%	Sedimentary Rock & Slate 35%
E36	Muddy Sand	Qtz, Green Minerals, Feldspar, 60%	Benthic Fora & Mollusca, Ostracod,10%	Sedimentary Rock 30%
E37	Clay	Qtz, Green Minerals, Biotite, 10%	Benthic Fora & Ostracod,80%	Sedimentary Rock 10%
E38	Clay	Qtz, 10%	Benthic Fora 85%	Sedimentary Rock 5%
E39	Muddy Sand	Qtz, Green & Light Green Minerals, 40%	Planktonic & Benthic Fora 30%	Sedimentary Rock & Slate 30%
E40	Sandy Mud	Qtz, Green & Light Green Minerals, 35%	Planktonic & Benthic Fora, Mullusca, Ostrocod, 50%	Sedimentary Rock & Slate 15%
E41	Sandy Mud	Qtz, Green & Light Green Minerals, 50%	Planktonic & Benthic Fora, Mullusca, Pteropod, 30%	Sedimentary Rock & Slate 20%
E42	Sandy Mud	Qtz,Feld, Light Green & Heavy Min. 40%	Planktonic & Benthic Fora, Mollusca, 40%	Sedimentary Rock & Slate 20%
E43	Muddy Sand	Qtz, Green & Light Green Minerals, 45%	Planktonic & Benthic Fora, Mullusca, Pteropod, 35%	Sedimentary Rock & Slate 20%
E44	Muddy Sand	Qtz, Green Minerals 60%	Planktonic & Benthic Fora, Mollusca, 20%	Sedimentary Rock & Slate 20%
E46	Medium-Coarse Sand	Qtz, Feld, Heavy Minerals, 40%	Planktonic & Benthic Fora, Mullusca, Ostrocod, 40%	Sedimentary Rock 20%

increase in the concentration with increasing water depth. The water in the middle of the study area contains high nitrite (more than 0.25 μmol), nitrate (more than 8 μmol) and phosphate (more than 0.6 μmol) near the 50-m mark (Chen and Bychkov, 1992). This high nutrient area mostly coincides with the high coccolith content area.

Table 3. List of calcareous nannoplankton in the East China Sea surface sediments.

Barrarudosphaera bigelowi (Gran and Braarud) Deflandre 1947
Calcidiscus leptoporus (Murray and Blackman) Loeblich and Tappan, 1978
Calcidiscus sp.
Coccolithus pelagicus (Wallich) Schiller, 1930
Coronosphaera binodata (Kamptner) Gaarder, 1977
Coronosphaera mediterranea (Lohmann) Gaarder, 1977
Crenalithus doronicoides (Black and Barnes) Roth, 1973
Cricolithus jonesi Cohen, 1965
Dictyococittes perplexa Burns, 1975
Dictyococittes productus (Kamptner) Backman, 1980
Dictyococittes sessilis (Lohmann) Biekart, 1989
Emiliania huxleyi (Lohmann) Hay and Mohler, 1967
Florisphaera profunda Okada and Honjo, 1973
Gephyrocapsa oceanica Kamptner 1943
(l - width larger than 3μm; m-width between 1-3μm)
small *Geophyrocapsa* (see Gartner, 1977)
Helicosphaera carteri (Wallich) Kamptner, 1954
Helicosphaera hyalina Gaarder, 1970
Helicosphaera neogranulata (Gartner) Chen, 1978
Helicosphaera pavimentum Okada and McIntyre, 1977
Helicosphaera wallichi (Lohmann) Okada and McIntyre, 1977
Oolithus fragilis (Lohmann) Okada and McIntyre, 1977
Pontosphaera messinae Bartolini, 1970
Pontoshpaera multipora (Kamptner) Roth, 1970
Syracosphaera lamina Lecal-Schlauder, 1951
Syracosphaera pulchra Lohmann, 1902
Syracosphaera sp.
Thorasosphaera heimi Lohmann, 1919
Thoracoaphaera tuberosa Kamptner, 1963
Umbellosphaera irragularis Paasche, 1955
Umbellosphaera tenuis (Kamptner) Paasche, 1955
Umbilicosphaera hulbertiana Gaarder, 1970
Umbilicosphaera laxus (Kamptner) Chen,1978
Umbilicosphaera sibogae (Weber-van Bosse) Gaarder, 1970

Wang and Samtleben (1983) recorded 40 species of calcareous nannoplankton, while Zhang and Siesser (1986) identified 36 taxa in the continental shelf sediments. In this study, 33 indigenous species and groups were found (Table 3). In the actual counting, reworked specimens and unidentified fragments were also counted as separate entities. *E. huxleyi* is the most dominant species, and its relative abundance varies from 26% at Station E46 to 72.3% at Station E17 (Figure 4). *G. oceanica* is also abundant in the surface sediments of the East China Sea Shelf, with its abundance varying from 14.7% at Station E17 to 44.7% at Station E46 (Figure 4). These two species account for more than 70% of the total flora observed in the surface sediments. The distribution of the two taxa, however, is markedly different. *E. huxleyi* concentrates in the central area, whereas *G. oceanic* spreads around

the four corners of the studied area (Figure 4). Small *Gephyrocapsa* is more common in the southern part, while the larger form of *G. oceanica* is more abundant in the northeastern part of the studied area (Figure 4).

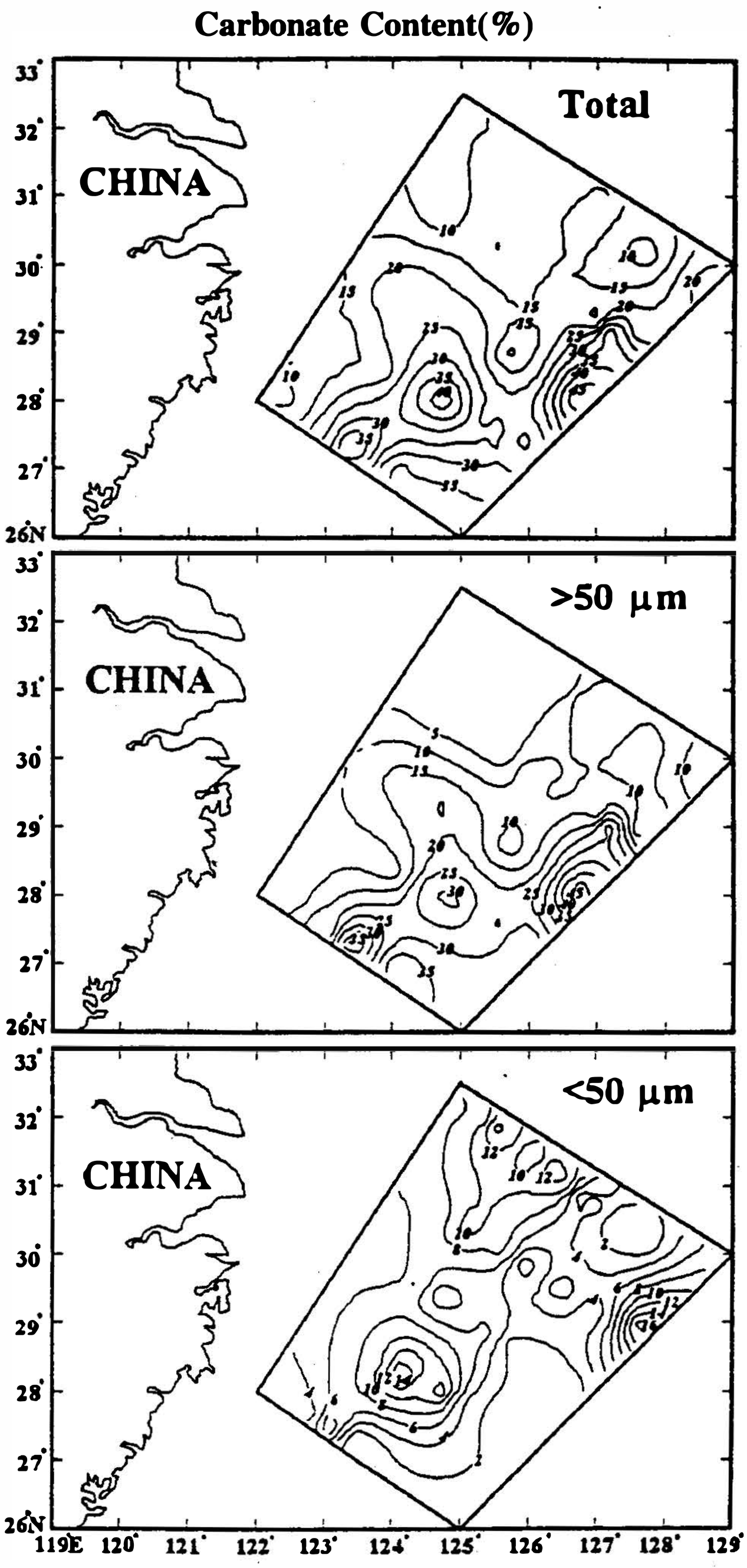

Fig. 3. Areal distributions of carbonate content of (1) the whole sediment (top), (2) with grain-size larger than 50 μm (middle), (3) with grain-size smaller than 50 μm (bottom).

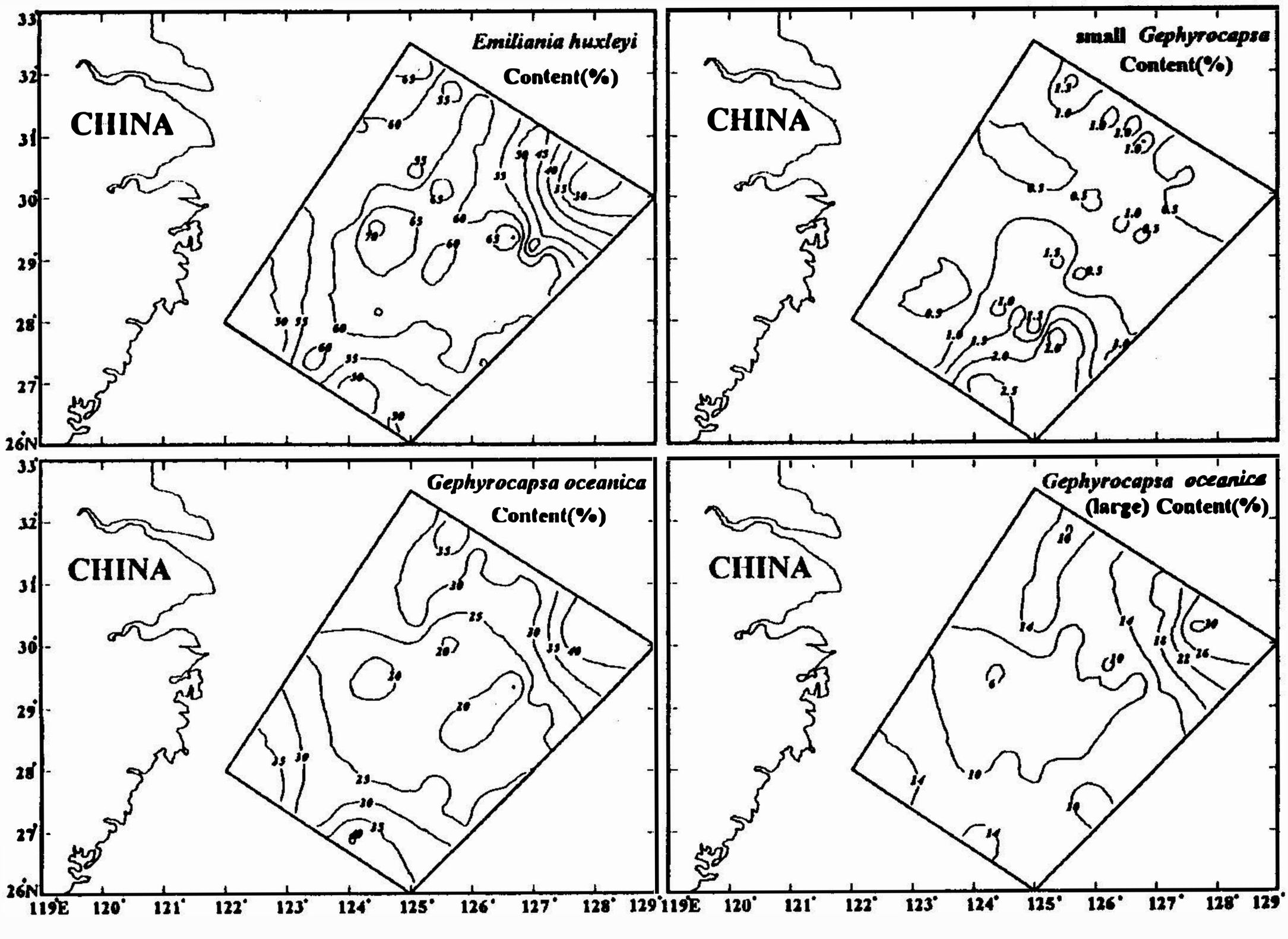

Fig. 4. Area distributions of relative abundance of four dominant calcareous nannoplankton spècies and groups.

5. NANNOFOSSILS FACTOR ANALYSIS

In order to gain an overview of cocolith distribution based on their relative abundances, the Q- mode factor analysis was applied. Ten species and groups (Table 4), with maxium abundances greater than 2% were studied. Three factors were chosen for this study. The distribution and characteristic species of these three factor loadings are shown in Figure 5 and are listed in Table 5.

Factor 1 is characterized by *E. huxleyi* and small *Gephyrocapsa*. The former exists in both warm-water and cold-water ecophenotypes (McIntyre and Bé, 1967; Okada and Honjo, 1973, 1975; Roth and Berger, 1975; Roth and Coulbourne, 1982). Both types occur on the East China Sea continental shelf. The ratio of the warm-to cold-water variety is about 1:1 in the inner-shelf and 10:1 in the outer-shelf sediments, reflecting the influence of the China Coastal Current and Kuroshio Current, respectively (Zhang and Siesser, 1986). Gartner (1988) indicated that the dominant small *Gephyrocapsa* assemblage may imply an abundant nutrient content and a low temperature in the photic water column. Therefore, Factor 1 may represent a water mass admixture which was brought by the Kuroshio Current, China Coastal Current and the Taiwan Current. The high loadings of Factor 1 are located in the northwest, middle and the southeast of the studied area (Figure 5). In these areas, the coccoliths were transported and deposited by the currents.

Table 4. List of calcareous nannoplankton taxa and their relative abundance used for factor analysis.

	Emiliania huxleyi	*Gephyrocapsa oceanica*	small *Gephyrocapsa*	*Dictyococcites productus*	*Florisphaera profunda*
E1	46	39	0.7	0	0.7
E2	45.7	36.4	0.7	0	0.7
E3	55	30	0.7	0	1.3
E4	63.3	24.4	0.7	0.3	0
E5	56.7	28.7	1.7	0.3	0
E6	47	38	2.7	0.3	0
E7	54.3	26.4	1	0.7	0
E8	66.6	18	2	2	0
E9	58.3	23.7	2.3	0.7	0
E10	60	24.7	3	0	0
E11	59.3	21	0.3	0.3	0.7
E12	63	21	2	1	0
E13	65.7	20	0.7	0	0.7
E14	61.7	23.3	1.3	0.3	1
E15	61.3	23.4	0.3	0	1.3
E16	56.7	20.7	1	0	4.3
E17	72.3	14.7	0.7	0	1.7
E18	69	18.3	1.3	0	0.7
E20	64	20.3	1.3	0.7	0.3
E21	54	23	1.7	0	4.3
E22	64.7	15	0.3	0.3	4.7
E24	64	20	1	0.3	0.7
E25	63.3	23	1	1	0
E26	45	27.3	0.7	1	4.3
E27	71.3	13.7	0.3	0.3	0
E28	65	19	1.3	0	0
E29	59.7	23.6	0.7	0.3	0.7
E30	58.3	21.3	0.3	0	3.7
E31	66	18.3	0.7	0	2.3
E32	66.7	21.3	0.3	0.3	1.7
E33	52	32	0.3	0	4.3
E35	59.3	28.7	0.3	0	2
E36	66.7	25.6	0.7	0	0.7
E37	54.3	38.3	1.7	0	1.7
E38	53.3	36	1.3	0	0
E39	65.3	26	0.7	0	1.3
E40	60	31	1.3	0.3	1.3
E41	57	31.3	0	0.3	2.3
E42	49	25.4	1.7	0	1.7
E43	49.7	27.6	0.3	0	0.7
E44	40	34.3	0.3	0	1
E45	31.7	41.5	0.7	0.7	0.7
E46	26	44.7	0	0	1

Table 4. (Continued)

	Helicosphaera carteri	*Helicosphaera wallichi*	*Thoracosphaera heimi*	*Thoracosphaera tuberosa*	*Umbilicosphaera sibogae*
E1	1	1	2	0.7	1.7
E2	0.3	0	0.7	2	1.7
E3	1	0	1	0.7	1.3
E4	1	0.3	0.3	1	1.3
E5	1	0	2	2	1.7
E6	1	1	1.7	1	1.3
E7	1.3	1.7	3.3	3.7	3
E8	1.6	0.3	1	2	2.6
E9	1	1	2	0.7	3
E10	0.7	0.7	2	0.7	3.3
E11	1.3	1	2	2.7	1
E12	1.7	1.7	1.3	0.7	1.7
E13	1	0	1.7	0.3	1.7
E14	1	1.3	0.7	1	1.3
E15	1	0.7	1	1.7	2.7
E16	0.7	1	2.3	1.3	1
E17	0.7	0	1.7	1.7	1.3
E18	0.3	1	0.7	0.3	1
E20	2.3	0.7	1.7	0	2.7
E21	2.7	0.7	1	2.7	1.3
E22	2	0.3	1.7	0.3	2.3
E24	1.3	0.7	1.3	0.3	2.3
E25	0.3	0.3	0.3	0.7	3
E26	3.7	0.7	4.7	1.3	5
E27	0.7	0.3	1.7	0.3	3
E28	2.3	1	1.7	0.3	2
E29	0.7	0.7	2.7	1.7	0.7
E30	1.7	1.3	1.3	0.7	2.7
E31	1	0.7	1.3	2	1.3
E32	1	1	0.3	0.3	1.3
E33	1.3	0.7	2.3	2.7	1
E35	1	1.3	1.7	2.3	0
E36	0.3	0.7	1.7	0.7	0.3
E37	0.3	0.7	0	0.7	0
E38	1	0.7	0.3	0.7	0.3
E39	0.7	0	1.3	0.7	1
E40	1.3	0.3	0.7	0	0.7
E41	1.3	0	1	0	2
E42	3	3	1	1.7	3
E43	1.7	0.7	3	2	4.3
E44	3	2	1.7	0.7	5
E45	3.9	1	6.9	1.6	2.6
E46	3.3	2	4.9	3.6	2

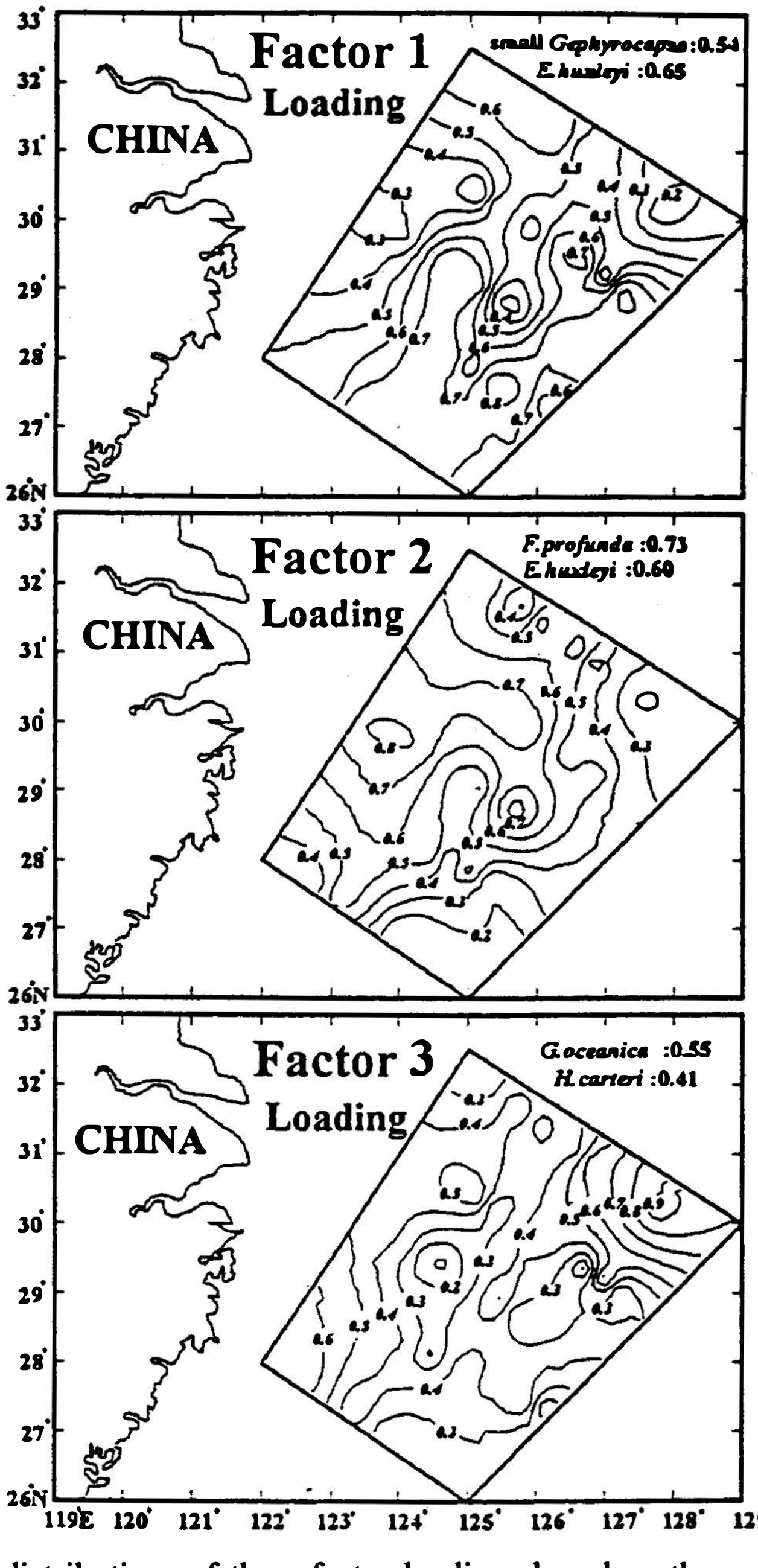

Fig. 5. Area distributions of three factor loadings based on the results of factor analysis.

Factor 2 is characterized by *E. huxleyi* and *F. profunda*. *F. profunda* is distributed from the shelf to the basin in the Pacific Ocean (Okada and Honjo, 1973). Its relative abundance increases gradually offshore and becomes very abundant at latitudes lower than 29°N (Tanaka, 1991). Both *E. huxleyi* and *F. profunda* are considered to be derived from

Table 5. Factor loadings of calcareous nannoplankton factor analysis of surface sediments in the East China Sea.

Station No.	Factor 1	Factor 2	Factor 3	Communality
E1	0.5356	0.3218	0.6922	0.8696
E2	0.4987	0.3585	0.5969	0.7335
E3	0.599	0.5884	0.4331	0.8926
E4	0.7948	0.4777	0.2796	0.9381
E5	0.7442	0.3189	0.4867	0.8924
E6	0.7388	0.0974	0.5726	0.8832
E7	0.5406	0.3134	0.6578	0.8232
E8	0.7559	0.2642	0.2839	0.7218
E9	0.8483	0.2383	0.3971	0.9341
E10	0.8318	0.2247	0.343	0.8600
E11	0.4947	0.5617	0.5041	0.8144
E12	0.8133	0.2773	0.3663	0.8725
E13	0.7226	0.6162	0.1694	0.9305
E14	0.7328	0.5186	0.3761	0.9474
E15	0.5464	0.6532	0.4407	0.9194
E16	0.2921	0.8162	0.3691	0.8877
E17	0.5655	0.7621	0.1339	0.9185
E18	0.7922	0.5488	0.0732	0.9341
E20	0.7658	0.3868	0.3383	0.8505
E21	0.2864	0.679	0.5403	0.8350
E22	0.2642	0.8698	0.2344	0.8813
E24	0.7684	0.5318	0.284	0.9539
E25	0.8338	0.3451	0.2048	0.8563
E26	0.2532	0.5237	0.659	0.7727
E27	0.7328	0.5304	0.0606	0.8220
E28	0.7431	0.4187	0.3435	0.8455
E29	0.6306	0.5491	0.4295	0.8836
E30	0.3142	0.7915	0.433	0.9127
E31	0.4854	0.7792	0.3249	0.9483
E32	0.6022	0.7232	0.2059	0.9281
E33	0.1613	0.7491	0.5948	0.9410
E35	0.3767	0.6638	0.5167	0.8495
E36	0.7	0.5846	0.2149	0.8779
E37	0.5924	0.4093	0.3935	0.6733
E38	0.7144	0.2612	0.4748	0.8040
E39	0.6545	0.669	0.2378	0.9325
E40	0.7073	0.4918	0.3321	0.8524
E41	0.4369	0.6757	0.3823	0.7936
E42	0.4484	0.3714	0.6685	0.7859
E43	0.4515	0.4239	0.6761	0.8407
E44	0.3554	0.2843	0.7544	0.7763
E45	0.2874	0.1667	0.8617	0.8529
E46	0.1185	0.2152	0.9469	0.9570
Eigenvalue	15.7359	11.9649	9.4990	37.1998
Percentage of total variance	36.5952	27.8253	22.0907	86.5112

the Pacific Ocean by the Kuroshio Current and its branch from the western part of the studied area. This trend may be explained by the trapping of these two species by the loop current off the Changjiang River. But, the Factor 2 loading distribution shows a high value near the estuary and the central part of the studied area (Figure 5). It is reasonable to believe that Factor 2 represents an admixture of a branch of the Kuroshio Current and a loop current off the Changjiang River.

Factor 3 is characterized by *G. Oceanica* and *H. carteri*, and its loading distribution shows a very high value near the northeast corner (Figure 5). *G. Oceanica* is most abundant in the coastal areas of Japan, particularly off the Choshi-Hachinohe area and along the east coast of Kyushun, where its relative abundance is higher than 60%, and it has a tendency to decrease with increasing distance from the coast (Tanaka, 1991). Although this species has a wide distributional range throughout the studied area, it is more concentrated at the NE corner (more than 40%) (Figure 5). This high concentration of *G. oceanica* implies that it may have been discharged by the longshore current from Japan. Factor 3 represents an influence of current from Japan.

6. GRAIN SIZE DISTRIBUTION OF SURFACE SEDIMENTS

From the distribution pattern of grain-size frequency (Figure 6), these sediments may be subdivided into four groups. Patterns A and D show unimodal distributions, whereas Patterns B and C demonstrate bimodel distributions (Figure 7). The mode peak of Pattern A is located at 6ϕ (16 μm) and 7ϕ (8 μm) and is mainly distributed in the northern corner of the studied area. A large patch of muddy sediment extends through the Bohai Sea into the Yellow Sea and reaches the East China Sea (Lee and Chough, 1989). Smaller mud areas are present off the estuary of the Changjiang River extending southward along the Chinese coast, and on the central shelf of the East China Sea at the south of Cheju Island. The fine particles deposited within the upper corner of the study area with a common carbonate content (Figure 3) represent the loess derived from the Yellow Sea.

The bimodal patterns B and C (Figure 7) are different from each other in two aspects. The coarse fraction in Pattern B is finer than that in Pattern C, and the finer fraction (finer than 63 μm) contains more abundant portions than Pattern C. These two patterns are spread between Patterns A and D. The grain size of the surface sediment decreases from the northern part toward the southern part.

Although Patterns A and D show unimodal distributions, the size distribution is concentrated within 1.5ϕ (350 μm) and 2.5ϕ (177 μm) which is markedly different from Pattern A showing the higher modes in fine to medium sand classes (Figure 7). This coarse material in Pattern D is composed of either terrigenous fine to medium sand or planktonic foraminifera.

The size distribution of the carbonate sediment shows three bimodal patterns (Figure 8). The size of loess ranges from 4ϕ (63 μm) to 12ϕ (0.24 μm) within the northern corner in Figure 8. In the southern corner, these three parts of biogenic sediments occur together (Figure 8). The size fraction larger than -0.5ϕ (1.41 mm) consists of shell fragments which are believed to be relict sediments in general. The size fraction between 0ϕ (1 mm) and 4ϕ (63 μm) is mainly composed of foraminifera, and the size smaller than 4ϕ (63 μm) consists mainly of coccoliths.

The distributions of siliciclastic sand, silt and clay are shown in Figure 9. With the exception of the northern corner, the sand content in the surface sediment of the study area

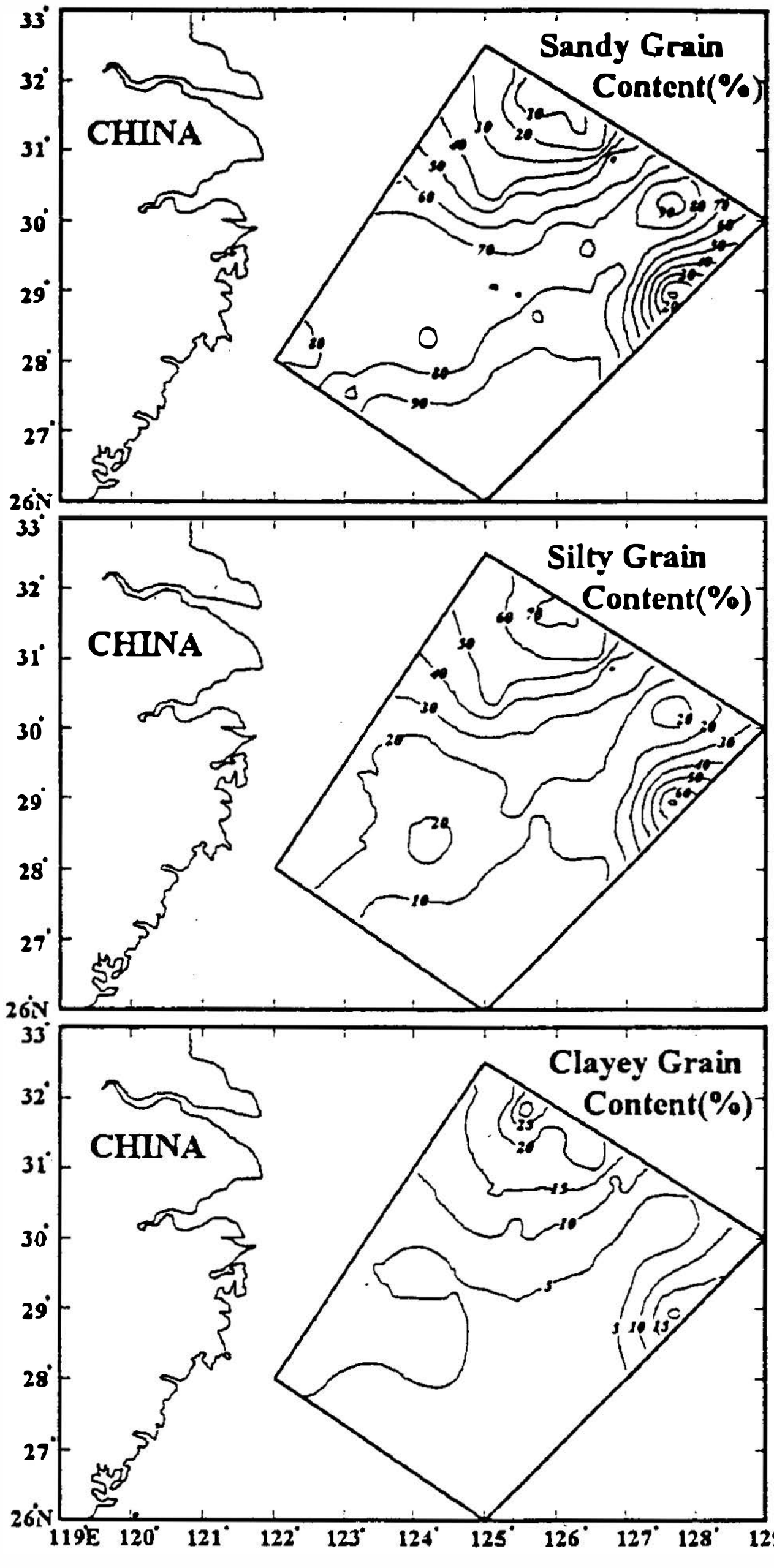

Fig. 6. Sand-, silt- and clay-sized distributions of the whole sediment.

is generally higher than 60%. The size distribution of this material also shows single and double modes (Figure 10). The single mode has its peak at the size class of 6ϕ (16 μm) to 7ϕ (8 μm), which may have been derived from the Yellow Sea. The coarse portion of the double mode pattern is quite abundant within two thirds of the study area. The sand size from 1ϕ (500 μm) to 3ϕ (125 μm) may have been not only transported from the

Total grain size histogram classification

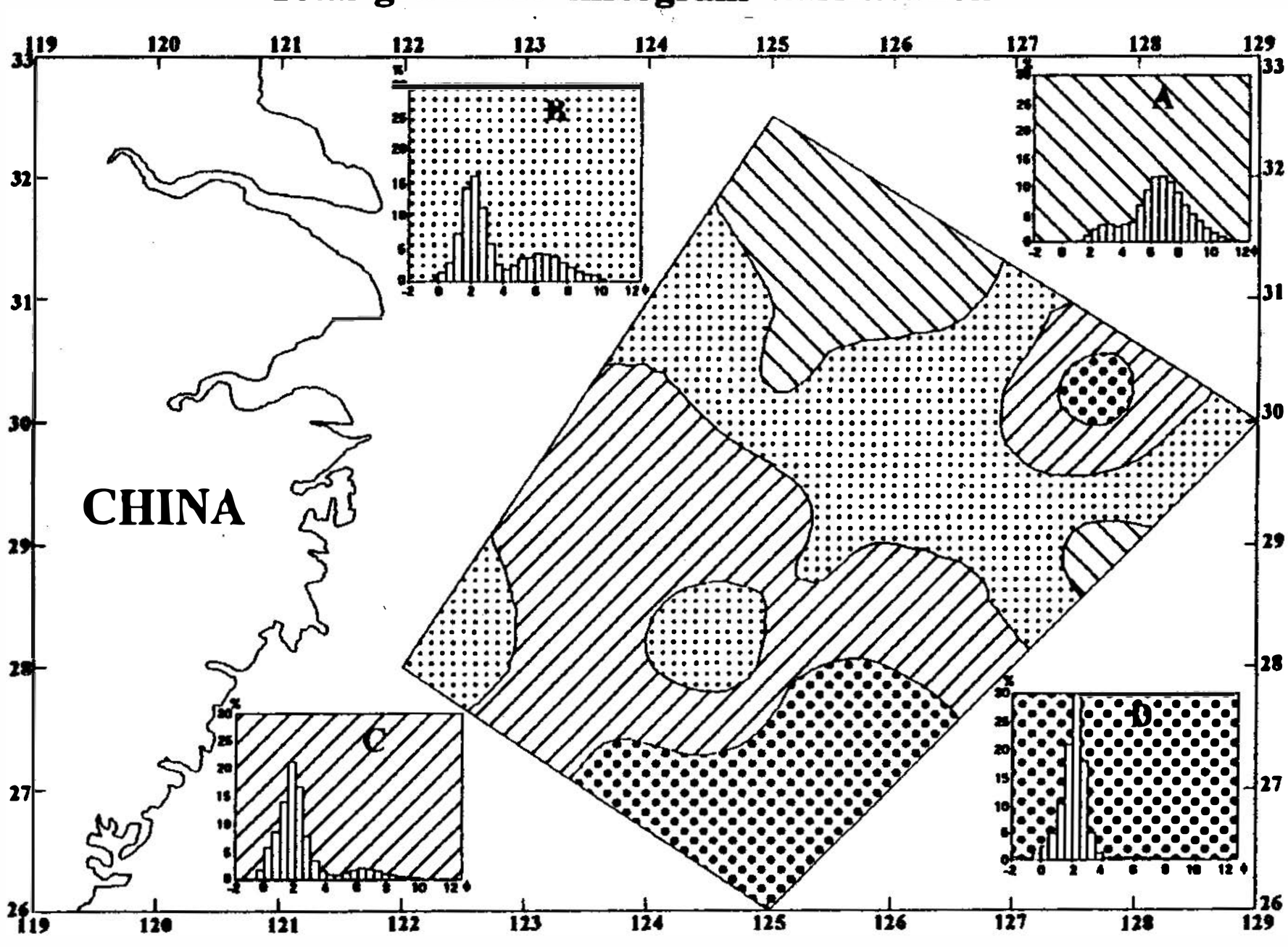

Fig. 7. Classification and geographic distribution of the grain-size frequency distribution of the whole sediment.

Carbonate grain size histogram classification

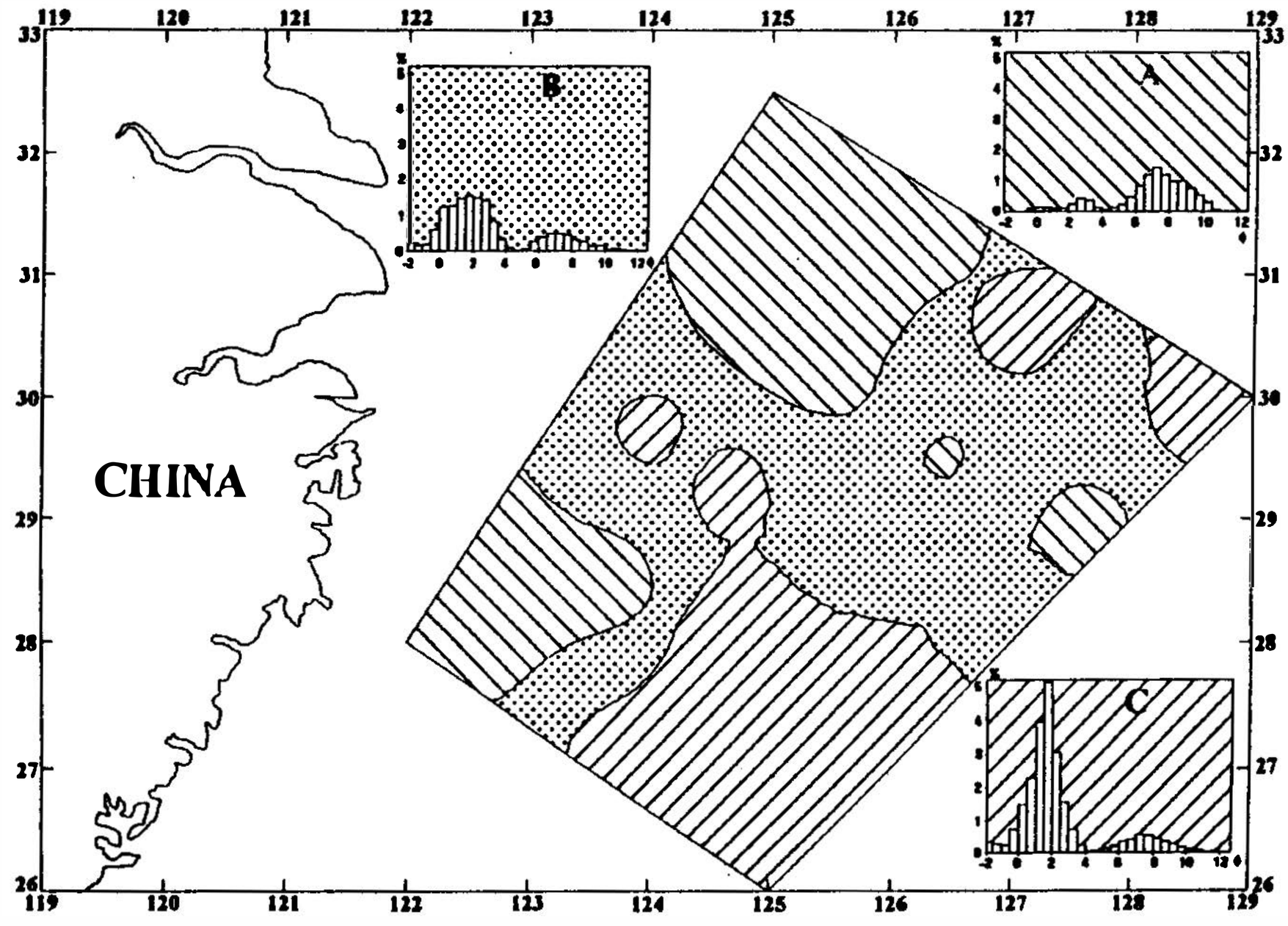

Fig. 8. Classification and geographic distribution of grain-size frequency distribution of the carbonate portions.

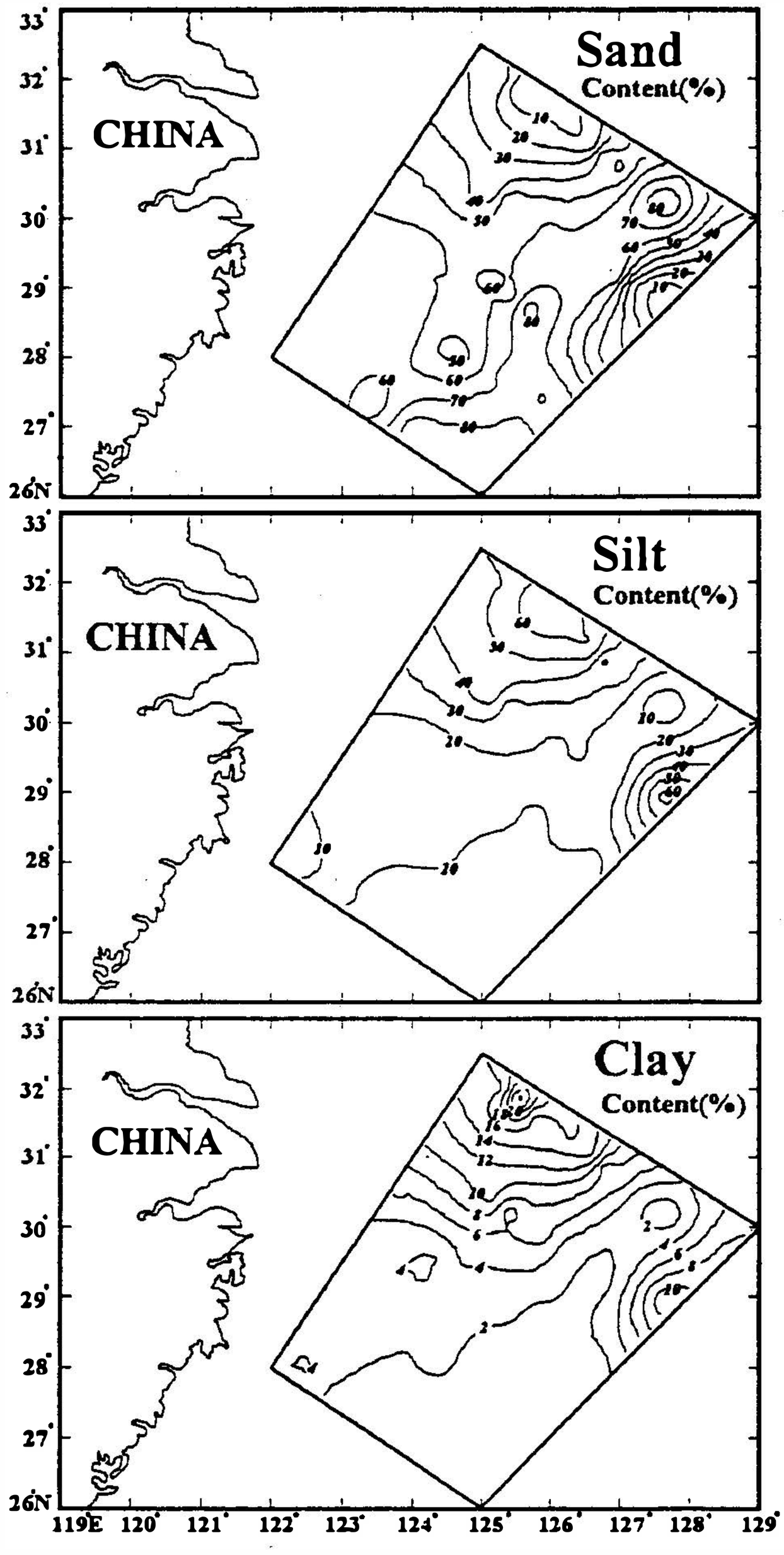

Fig. 9. Area distributions of clastic sand, silt and clay.

Changjian River but also may have been dispersed from Taiwan island by either the Taiwan Current in the west or the Kuroshio Current in the east.

7. CURRENT PATTERN ON THE EAST CHINA MIDDLE AND OUTER SHELVES

The floral assemblage of coccoliths and the grain-size distributions in the surface sediment are indicators of the sediment transport in suspension and bed load. The loess

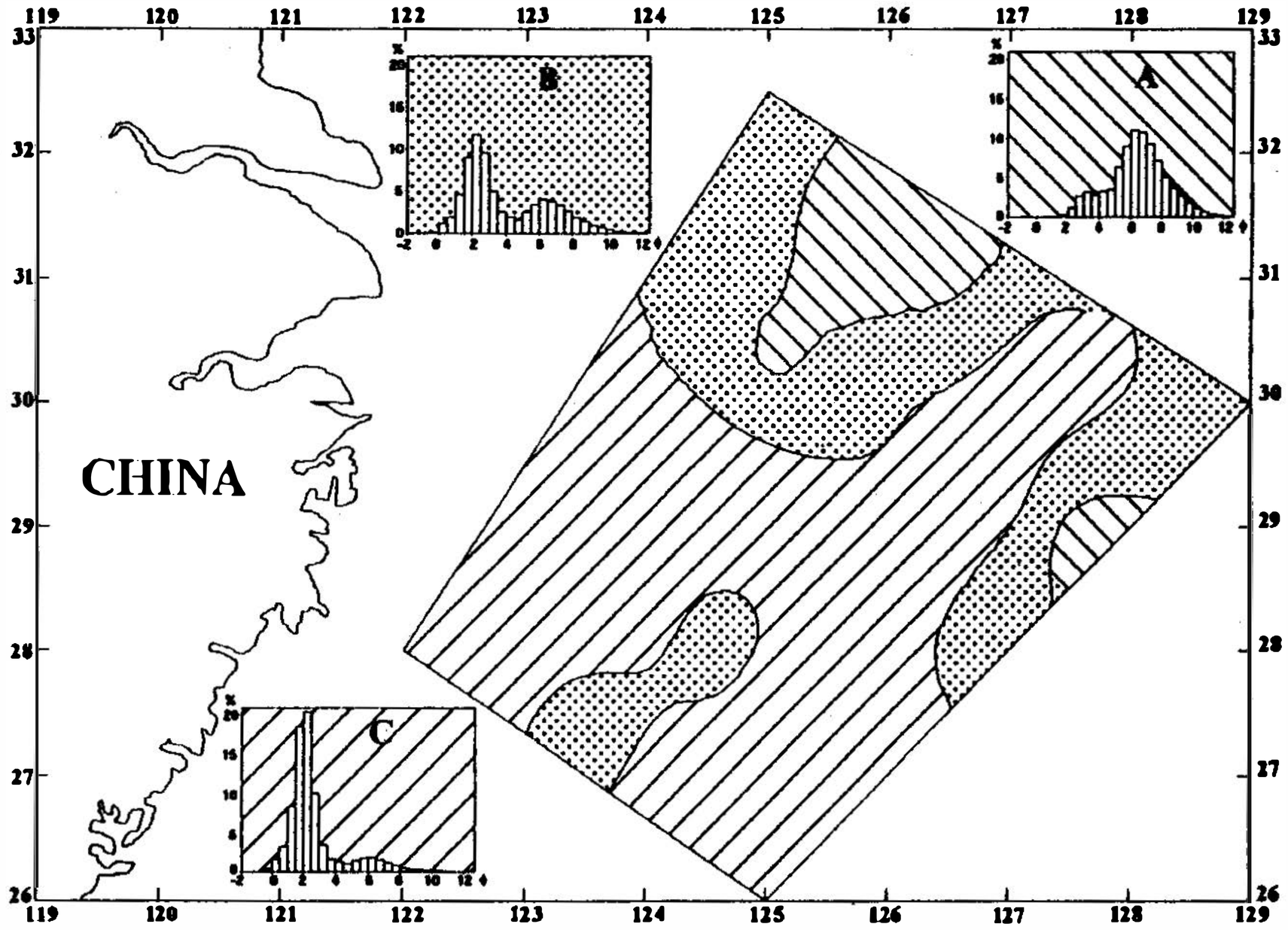

Fig. 10. Classification and geographic distribution of the grain-size frequency distribution of the clastic portion (non-carbonate sediment).

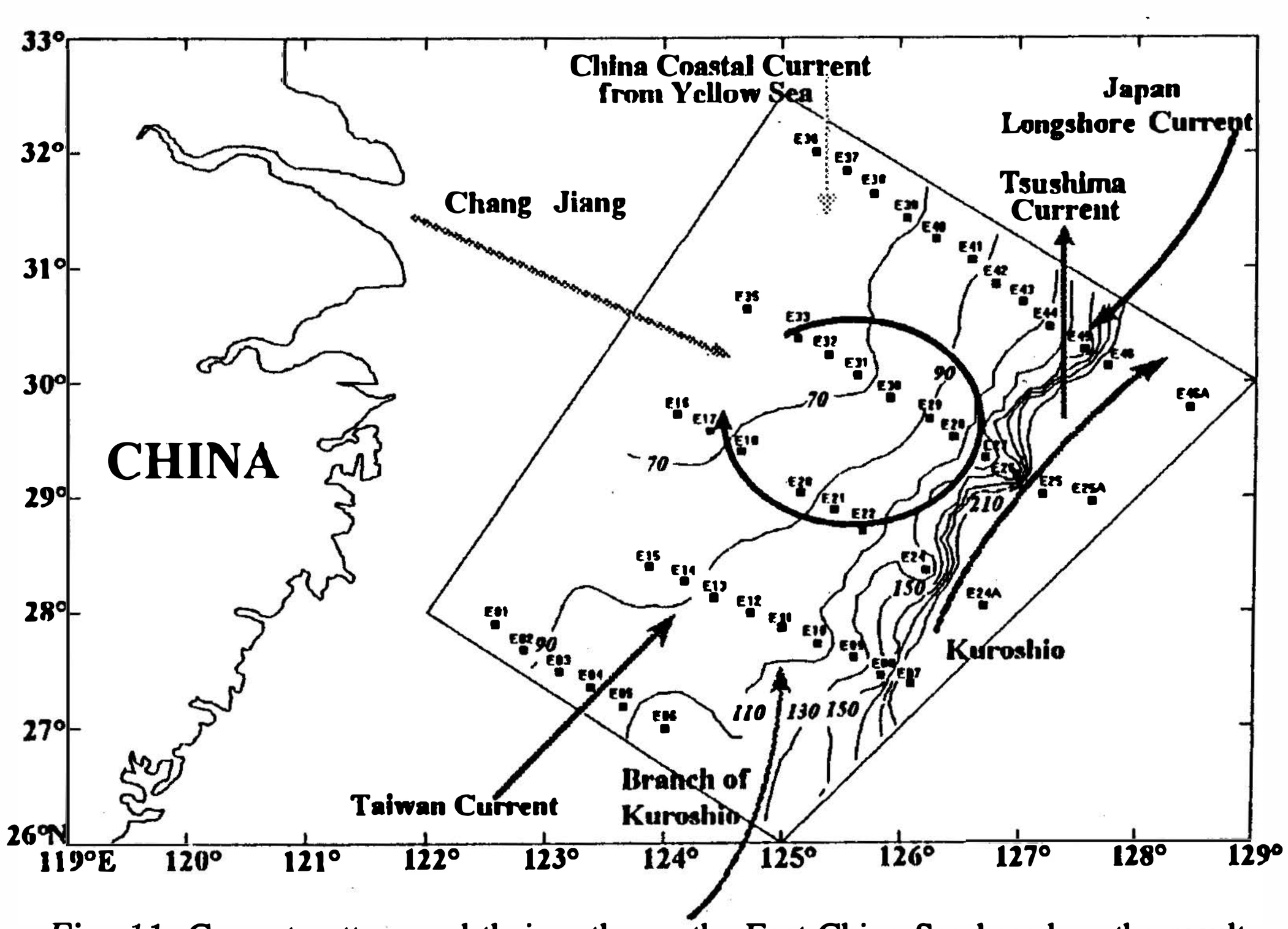

Fig. 11. Current pattern and their paths on the East China Sea based on the result of this study.

distribution indicates that material from the Huanghe may have been transported by the China Coastal Current from the Bohai and Yellow Seas to as far south as 31.5°N (Figure 10). Although most of the suspended sediment from the Changjiang River is deposited at the vicinity of the river mouth or was transported to the south, the particles dispersed eastward are taken up in the large gyre on the middle and outer shelves. The eastward transport occurs during high river flooding in the summer season (Yun *et al.*, 1981). Landsat images show a marked turbid flow to the north northeast of the river mouth during that period (Yun *et al.*, 1981). The gyre on the shelf consists of a branch of the Taiwan Current from the south and a branch of the Kuroshio Current from the southeast. These branches supply sediment from the west and north coast of Taiwan (Chen, *et al.*, 1992). The sediment from the Pacific Ocean is entrapped in the center of the gyre.

The main branch of the Kuroshio Current passes the east side of the shelf break and flows into the Okinawa Trough. Another branch of the Kuroshio Current becomes the Tsushima Current of the Japan Sea. They separate at about 30.7°N between the Kuroshio and Tsushima Currents, the sediment is dispersed by the longshore current from the offshore area of the Japanese east coast (Figure 11).

Figure 11 gives the general circulation pattern with some seasonal variations. Dispersal along the bottom may differ from dispersal through the surface water. On the basis of the tides alone, Dong *et al.* (1989) calculated that a pattern of areas of divergence and convergence exists in the Yellow Sea with currents directed mainly southward. Cai (1982) indicated that the amount of Changjiang River suspended matter going eastward is very small because the concentration in the eastward flow is on the order of 6 mg/l while that of the southward flow is about 500 mg/l.

8. CONCLUSIONS

Analysis of the calcareous nannofossil assemblage, carbonate content and grain size distributions on the middle to outer shelves of the East China Sea middle indicates seven current paths: the Kuroshio Current, a branch of the Kuroshio, the Taiwan Current, the loop current off the Changjiang River, the China Coastal Current, the Tsushima Current and the longshore current from Japan. The grain-size distribution of sediment discharged from the Yellow Sea is characterized by a higher portion of fine sediment. The sediment along the shelf break is composed of coarse mollusca fragments and foraminifera. A bimodal distribution pattern occurs between those single mode areas indicating the admixture of loess, terrigenous material and biogenic matters.

Acknowledgments The authors would like to thank Drs. Stefan Gartner, Hisatake Okada, George T. F. Wong, Yuan-Hui Li and Su Jilan for reviewing drafts of this manuscript and for discussions which greatly improved the final version. This study is supported by the National Science Council of the ROC, Grant NSC-82-0209-M002a-11-K and NSC-82-0209-M002a-17-K. The authors are also grateful to Dr. A. Bychkov, Mr. T. T. Liu and crew members of *R/V Vinogradov* for their assistance with the field work.

REFERENCES

Cai, A., 1982: Diffusion of sediments of the Changjiang River discharging into the sea. *Acta Oceanol. Sinica*, **4**, 78-88.

Chen, M. P., S. C. Lo, and K. L. Lin, 1992: Composition and texture of surface sediment indicating the depositional environments off northeast Taiwan. *TAO*, **3**, 395-418.

Chen, M. P., and A. Bychkov, 1992: ROC-Russia Marine Science Collaboration Project-KEEPMASS Initial Data Report. National Science Council of the ROC and the Russian Academy of Sciences. 444pp.

Chern, C. S., J. Wang, and D. P. Wang, 1990: The exchange of Kuroshio and East China Sea shelf water. *J. Geophys. Res.*, **95**, 16017-16023.

Chu, T. Y., 1971: Environmental study of the surrounding waters of Taiwan. *Acta Oceanogr. Taiwanica*, **1**, 15-31.

Dong, L., J. Su, and K. Wang, 1989: The relationship between tidal current field and sediment transport in the Huang Hai Sea and the Bohai Sea. *Acta Oceanol. Sinica*, **8**, 587-600.

Fan, K. L., 1985: STD measurements in the seas around Taiwan during 1977-1983, Institute of Oceanography, National Taiwan University, Special Publication 44., 337pp.

Fincham, M. J., and A. Winter, 1989: Paleoceanographic interpretations of coccoliths and oxygen-isotopes from the sediment surface of the southwest Indian Ocean. *Marine Micropaleont.*, **13**, 326-351.

Gartner, S., 1977: Calcareous nannofossil biostratigraphy and revised zonation of the Pleistocene. *Marine Micropaleont.*, **2**, 1-25.

Gartner, S., 1988: Paleoceanography of the mid-Pleistocene. *Marine Micropaleont.*, **13**, 23-46.

Geitzenauer, K., M. B. Roche, and A. McIntyre, 1976: Modern Pacific Coccolith Assemblages: Derivation and Application to Late Pleistocene Paleotemperature Analysis. In: Cline R. M. and J. D. Hays, (Eds.), Investigation of Late Quaternary paleoceanography and paleoclimatology. *Geol. Soc. Am., Mem.*, **145**, 423-448.

Lee, H. J., and S. K. Chough, 1989: Sediment distribution, dispersal and budget in the Yellow Sea. *Mar. Geol.*, **87**, 195-205.

Li, C., G. Chen, M. Yao, and P. Wang, 1991: The influences of suspended load on the sedimentation in the coastal zones and continental shelves of China. *Mar. Geol.*, **96**, 341-352.

Loubere, P., 1982: Plankton ecology and the paleoceanographic climatic record. *Quat. Res.*, **17**, 314-324.

McIntyre, A., and A. W. H. B, 1967: Modern coccolithophoridae of the Atlantic Ocean- I. Placolith and cyrtoliths. *Deep-Sea Res.*, **14**, 561-597.

McIntyre, A., A. W. H. B, and M. B. Roche, 1970: Modern Pacific coccolithophorida: A paleontological thermometer. *New York Acad. Sci., Trans., Ser.*, 2, **32**, 720-731.

Molnia, B. F., 1974: A rapid and accurate method for the analysis of calcium carbonate in small samples. *J. Sed. Petrol.*, **44**, 589-590.

Okada, H., and S. Honjo, 1973: The distribution of oceanic coccolithphorida in the Pacific. *Deep-Sea Res.*, **20**, 355-374.

Okada, H., and S. Honjo, 1975: Distribution of coccolithophores in marginal seas along the western Pacific Ocean and in the Red Sea. *Mar. Biol.*, **31**, 271-285.

Qin, Y., and F. Li, 1983: Study of the influence of sediment loads discharged from the Huanghe River on sedimentation in the Bohai Sea and Huanghai Sea. Proc. Int'l Symposium Sedimentation Continental Shelf with Special Reference to the East China Sea. China Ocean Press. 83-92.

Roth, P. H., and W. H. Berger, 1975: Distribution and dissolution of coccoliths in the South and central Pacific. In: W. V. Sliter, A. W. Bé and W. H. Berger, (Eds.), Dissolution of Deep-Sea Carbonates. Cushman. Found. Foram. Res., Special Publication 13, 87-113.

Roth, P. H., and W. T. Coulbourn, 1982: Floral and solution patterns of coccoliths in surface sediments of the North Pacific. *Marine Micropaleont.*, **7**, 1-52.

Tanaka, Y., 1991: Calcareous nannoplankton thanatocoenoses in surface sediments from seas around Japan. *Sci. Rep., Tohoku Univ., 2nd ser. (Geol.)*, **61**, 127-198.

Wang, P., and Q. Min, 1981: A preliminary study of calcareous nannoplankton in bottom sediments of the East China Sea. *Acta Oceanol. Sinica*, **3**, 188-192.

Wang, P., and C. Samtleben, 1983: Calcareous nannoplankton in surface sediments of the East China Sea. *Marine Micropaleont.*, **9**, 249-259.

Winter, A., 1985: Distribution of living coccolithophores in the California Current system, southern California borderland. *Marine Micropaleont.*, **9**, 385-393.

Yang, Z., and J. D. Milliman, 1983: Fine-grained sediments of the Changjiang and Huanghe Rivers and sediment sources of the East China Sea. Proc. Int'l Symposium Sedimentation Continental Shelf with Special Reference to the East China Sea. China Ocean Press. 405-415.

Yun, C., M. Cai, and B. Wang, 1981: An analysis of the diffusion of suspended sediment discharged from the Changjiang River based on satellite images. *Oceanol. Limnol. Sinica*, **12**, 391-401.

Zhang, J., 1988: Calcareous nannoplankton in the surface sediments of the East China Sea and its environmental implications. *Acta Oceanol. Sinica*, **7**, 266-286.

Zhang, J., and G. Siesser, 1986: Calcareous nannoplankton in continental-shelf sediments, East China Sea. *Marine Micropaleont.*, **32**, 271-281.

Zhu, E., and O. Wang, 1988: Sedimentation on the north shelf of the East China Sea. *Mar. Geol.*, **81**, 123-136.